BIOCHEMISTRY

 Volume 43, Number 32 August 17, 2004

Accelerated Publications

Mechanistic Studies of a Flavin-Dependent Thymidylate Synthase†

Nitish Agrawal,§ Scott A. Lesley,‡ Peter Kuhn,⊥ and Amnon Kohen*,§

Department of Chemistry, University of Iowa, Iowa City, Iowa 52242, Genomics Institute of the Novartis Research Foundation, 10675 John Jay Hopkins Drive, San Diego, California 92121, and The Scripps Research Institute, CB265, 10550 North Torrey Pines, La Jolla, California 92037

Received May 11, 2004; Revised Manuscript Received June 19, 2004

ABSTRACT: The *ThyA* gene that encodes for thymidylate synthase (TS) is absent in the genomes of a large number of bacteria, including several human pathogens. Many of these bacteria also lack the genes for dihydrofolate reductase (DHFR) and thymidine kinase and are totally dependent on an alternative enzyme for thymidylate synthesis. *Thy1* encodes flavin-dependent TS (FDTS, previously denoted as TSCP) and shares no sequence homology with classical TS genes. Mechanistic studies of a FDTS from *Thermotoga maritima* (TM0449) are presented here. Several isotopic labeling experiments reveal details of the catalyzed reaction, and a chemical mechanism that is consistent with the experimental data is proposed. The reaction proceeds via a ping-pong mechanism where nicotinamide binding and release precedes the oxidative half-reaction. The enzyme is primarily pro-*R* specific with regard to the nicotinamide (NADPH), the oxidation of which is the rate-limiting step of the whole catalytic cascade. An enzyme-bound flavin is reduced with an isotope effect of 25 (consistent with H-tunneling) and exchanges protons with the solvent prior to the reduction of an intermediate methylene. A quantitative assay was developed, and the kinetic parameters were measured. A significant NADPH substrate inhibition and large K_M rationalized the slow activity reported for this enzyme in the past. These and other findings are compared with classical TS (*ThyA*) catalysis in terms of kinetic and molecular mechanisms. The differences between the FDTS proposed mechanism and that of the classical TS are striking and invoke the notion that mechanism-based drugs will selectively inhibit FDTS and will not have much effect on human (and other eukaryotes) TS. Since TS activity is essential to DNA replication, the unique mechanism of FDTS makes it an attractive target for antibiotic drug development.

Deoxythymidine 5′-monophosphate (dTMP)[1] is one of the four building blocks of DNA. Until recently, dTMP in all cellular organisms was thought to be formed de novo by thymidylate synthase (TS, encoded by *ThyA*). TS catalyzes the reductive methylation of deoxyuridine 5′-monophosphate (dUMP) to form dTMP (*1*). Classical TSs use *R*-N^5,N^{10}-

† This work was supported by NIH Grant R01 GM65368-01 and NSF Grant CHE-0133117 to A.K. and the NIH NIGMS Protein Structure Initiative (Grant GM59965-02) to P.K.

* Corresponding author. Tel: 319-335-0234. Fax: 319-335-1270. E-mail: amnon-kohen@uiowa.edu.

§ University of Iowa.

‡ Genomics Institute of the Novartis Research Foundation.

⊥ The Scripps Research Institute.

[1] Abbreviations: FDTS, flavin-dependent thymidylate synthase (previously denoted as TSCP); KIE, kinetic isotope effect; RP HPLC, reverse phase high-pressure liquid chromatography; LSC, liquid scintillation counter; dUMP, 2′-deoxyuridine-5′-monophosphate; dTMP, 2′-deoxythymidine-5′-monophosphate; CH_2H_4folate, *R*-N^5,N^{10}-methylene-5,6,7,8-tetrahydrofolate; H_2folate, 7,8-dihydrofolate; H_4folate, 5,6,7,8-tetrahydrofolate; FAD, flavin adenine dinucleotide; Mdpm, million decompositions per min.

10.1021/bi0490439 CCC: $27.50
Published on Web 07/20/2004

methylene-5,6,7,8-tetrahydrofolate (CH_2H_4folate) both as a methylene donor and as a reductant (hydride donor) leading to 7,8-dihydrofolate (H_2folate) formation (*2*). Because 5,6,7,8-tetrahydrofolate (H_4folate) and its derivatives are essential for a variety of biological processes, H_2folate formed by TS is rapidly reduced to H_4folate by dihydrofolate reductase (DHFR). This coupling of TS and DHFR proteins was thought to be essential for de novo thymidylate synthesis in virtually all dividing cells (*1*). Recently, several organisms were identified that lack *ThyA* in their genome (*3*). Most of these also lack genes for DHFR and thymidine kinase (an enzyme that enables salvage of thymidine derivatives from the growth media), suggesting that an alternative TS activity must be present. A new family of genes was identified that encodes for enzymes that convert dUMP to dTMP via an alternative pathway (*4*). These genes are called *Thy1* (or *ThyX*) and are widely distributed in bacterial and archaeal organisms including several human pathogenic bacteria (*3*, *4*). This alternative TS is named TS complementing protein (TSCP) (*3*) or flavin-dependent TS (*5*) (denoted below as FDTS). Since it has no sequence homology with TS, drugs targeting FDTS may be specific to those pathogens with little, if any, toxic effect in humans. Development of such drugs would greatly benefit from understanding of the FDTS catalytic mechanism, the reactants binding order, and identification of the rate-limiting step, intermediates, and possible transition states (of which analogues may lead to the most promising inhibitors).

Classical TSs have been extensively studied in terms of structure, kinetics, and mechanism. They are among the most highly conserved enzymes with approximately 18% of residues strictly conserved (*2*). Numerous X-ray structures of free TS and bound enzyme−substrate−cofactor analogues have been determined, and several hundred mutants have been cloned and studied (*2*). The mechanism of classical TS is relatively well understood, and mechanism-based drugs are in extensive clinical use (e.g., 5-fluorouracil). The in-depth studies included investigation of environmentally coupled hydrogen tunneling in the hydride transfer step (*6*) and the functional dynamics of the protein (*7*). The mechanism of the FDTS, on the other hand, is not yet well understood (*3*, *4*). The crystal structure of FDTS from *Thermotoga maritima* (TM0449) was solved by Kuhn et al. in 2002 (*8*). This is a tetramer with four identical subunits with a molecular weight of 26005 Da each (220 amino acid residues), and no structural similarities are apparent between FDTS and classical TS. Recently, Mathews et al. (*3*) have shown an absolute activity dependency on flavin adenine dinucleotide (FAD), CH_2H_4folate, and reduced nicotinamide adenine dinucleotide (NAD(P)H). The activity assay used by Mathews et al. was based on a qualitative thin-layer chromatography (TLC) analysis of [2-^{14}C]-dUMP. Yet that assay indicated that NADPH enhances the enzyme activity better than NADH. Accordingly, NADPH was used in the current work. In ref *3*, eight crystal structures of TM0449 were solved with several ligands (including FAD, dUMP, and 5-fluoro-dUMP). These structures clearly identified the FAD and dUMP binding sites. Structural features that directly affect the current study include the following: (i) the adenine-pyrophosphate moiety of the FAD is anchored (noncovalently) deep inside the protein, while its reactive isoalloxazine ring is exposed to the protein surface and appears to be fairly flexible; (ii) there is no space for the adenine-pyrophosphate moiety of NADPH in the monophosphate ribose binding pocket of dUMP; (iii) the (*p*-aminobenzoyl)-glutamate moiety of CH_2H_4folate has no apparent binding pocket close to the dUMP with or without bound FAD; (iv) the only nucleophile in the active site is Ser88, which is about 4 Å from the flexible pyrimidine ring of dUMP. This serine is at position 84 of FDTS from *Helicobacter pylori* for which either the mutants at Ser84 are inactive or their activity is partly rescued by Ser85 (for which glycine is present for the TM0449 enzyme), indicating a critical role of this serine in catalysis (*5*). The analogy that springs to mind is the dichotomy between serine proteases and cysteine proteases: the OH and SH nucleophile contrast is present there too.

In this paper, we present an experimental analysis of isotopically labeled reactants and products and a spectroscopic investigation of the TM0449-encoded FDTS. The experimental data and computer modeling shed light on the FDTS-catalyzed reaction and suggest a kinetic and chemical mechanism for the function of the enzyme. The stereospecificity, H-tunneling contribution, and other mechanistic features of the enzyme are also discussed and compared to the classical TS (*ThyA*).

MATERIALS AND METHODS

Materials

dUMP, dTMP, NADPH, dithiothreitol (DTT), Tris(hydroxymethyl)aminomethane, and $MgCl_2$ were from Sigma Co. CH_2H_4folate was a generous gift from Eprova Inc, Switzerland. The syntheses of *R*-[6-^{3}H]-CH_2H_4folate, *R*-[4-^{3}H]-NADPH, and *S*-[4-^{3}H]-NADPH have been described in detail elsewhere (*9*−*12*). [2-^{14}C]-dUMP (specific radioactivity, 52 Ci/mol) was from Moravek Biochemicals. Ultima Gold liquid scintillation cocktail and liquid scintillation vials were from Packard Bioscience. The FDTS enzyme (TM0449, GeneBank accession number NP228259) was expressed and purified as previously described (*8*).

Methods

Analytical Methods. Liquid scintillation counter (LSC) Tri-Carb model 2900 TR from Packard Bioscience was used. The HPLC system used was Agilent Technologies (previously HP) model 1100 equipped with an online degasser, a quaternary pump, a temperature-controlled column chamber, an UV/vis diode array detector, and a manual injector. The column (C18, 250 mm × 4.6 mm, 5 μm, Discovery series) was from Supelco, and the column temperature was maintained at 25 °C. All analytical procedures are published in detail elsewhere (*10*, *11*). The HPLC was followed by a fraction collector (1 min per fraction), and the fractions were counted for 5 min each by LSC.

Studies with Labeled Substrates. All experiments were performed at 37 °C in 200 mM Tris buffer, pH = 8.0, 10 mM $MgCl_2$, 1 mM DTT, 5 mM CH_2O (to maintain constant CH_2H_4folate concentration), and 0.5 mM each of NADPH, dUMP, and CH_2H_4folate. Prior to each experiment, a trace amount of tritiated substrate (*R*-[6-^{3}H]-CH_2H_4folate, *R*-[4-^{3}H]-NADPH, or *S*- [4-^{3}H]-NADPH), and 7.5 μM of [2-^{14}C]-dUMP were added (typically 1.5 Mdpm tritium and 0.5

Mdpm ^{14}C). The ^{14}C-labeled dUMP was used to follow the progress of the reaction, and all experiments were done in triplicate. The reaction was initiated by addition of 2.4 μM FDTS (9.6 μM active sites using $\epsilon_{454} = 12.5$ mM^{-1} cm^{-1} per flavin), and aliquots were withdrawn at various times. These aliquots were analyzed by reverse phase HPLC followed by both UV/vis diode array and fraction collector. The collected fractions were analyzed by LSC for ^{14}C and T simultaneously. All the relevant standard materials were tested, and three different RP HPLC methods (developed in our lab (*10, 11*)) were used to facilitate the analysis of all reactants and products. Experiments in which air-sensitive intermediates (e.g., H_4folate) had to be stabilized were repeated in strict anaerobic conditions under argon (Ar).

Electron Spray Mass Spectrometry (ESMS). To test the source of the hydride that reduces the methylene intermediate to form the methyl group of dTMP, the reaction was conducted in a H_2O/D_2O mixture (~50/50) utilizing the same reaction composition and conditions as those described above. The reaction mixture was analyzed after 1 h by an electron spray mass spectrometer (Micromass, Inc., Autospec, a high-resolution mass spectrometer). Samples were filtered through Centricell 20 (10000 NMWL) to remove the protein and lyophilized prior to ESMS analysis.

Enzyme−FAD Reduction by NADPH. To test whether enzyme−FAD reduction requires any other substrate except NADPH (e.g., dUMP, CH_2H_4folate, or both), 2.5 μM enzyme (as it was isolated with bound FAD in its yellow oxidized state) was incubated with an excess of NADPH (1 mM) in 200 mM Tris buffer, pH = 8, under Ar, and the 340 and 454 nm absorbances of NADPH and FAD were followed by a UV/vis spectrophotometer.

NADPH Concentration Dependence of Initial Rates. Initial velocities of TM0449 were measured by following the formation of ^{14}C-labeled dTMP from dUMP. To investigate the reaction rate dependence on NADPH concentration, the reaction was conducted with NADPH concentrations varying from 10 to 1500 μM with fixed 100 μM dUMP (including 15 μM [2-^{14}C]-dUMP), and 500 μM CH_2H_4folate. The reaction mixture contained 200 mM Tris buffer (pH = 8.0), 10 mM $MgCl_2$, 5 mM CH_2O, and 1 mM DTT and was preincubated under argon at 37 °C. The reaction was then initiated by addition of 2.5 μM FDTS (10 μM active sites using $\epsilon_{454} = 12.5$ mM^{-1} cm^{-1} per flavin), and aliquots were withdrawn at early time points (percentage conversion of 2−15%). These aliquots were analyzed by reverse phase HPLC and followed by radioactive flow detector. The rate was calculated from the fractional conversions at three or four different time points.

Computer Modeling and Docking. NADPH and CH_2H_4-folate cofactors were constructed using standard geometric parameters of the molecular modeling software package SYBYL, version 6.9/6.7 (Tripos Inc., St. Louis, MO). Atomic charges were calculated using the Gasteiger−Huckel protocol.

To test the feasibility of NADPH binding to the TM0449−FAD complex and its capability to reduce the flavin, dUMP was deleted from the crystal structure of the TM0449−FAD−dUMP ternary complex (PDB entry 1O26). Then, the Tripos force field was used to dock NADPH into the pyrimidine original binding pocket.

Scheme 1: An Illustration of the Chemical Similarities between Methylated Pterin (in gray) and the Isoalloxazine Moiety (in black)[a]

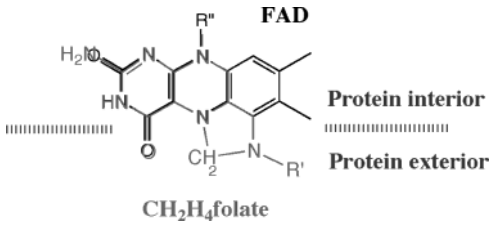

CH_2H_4folate

[a] The flavin binds with its adenosine-5′-pyrophosphate-ribityl moiety (R″) at the interior of the protein, while CH_2H_4folate fits with the (*p*-aminobenzoyl)-glutamate moiety (R′) at the exterior of the protein.

To test the feasibility of CH_2H_4folate binding to the TM0449−FAD−dUMP complex and delivering a methylene to the C-5 position of dUMP, we started from the 1O26 PDB coordinates and moved the isoalloxazine ring to an open cavity by rotating the 2′−3′ bond of the flavin FMN moiety. This type of FAD conformational change has been observed in several flavo-enzymes in the past (*13*−*15*). The original coordinates of the isoalloxazine were then used to construct the pterin ring of the CH_2H_4folate (Scheme 1).

RESULTS AND DISCUSSION

The Hydride Transfer Path and Kinetics. To elucidate the source and path of the hydride that leads to the reduction of the single carbon methylene group, the FDTS reaction was conducted using substrates that were tritium-labeled at various positions. The conversion of [2-^{14}C]-dUMP to [2-^{14}C]-dTMP was used to follow the progress of the protonated substrates. The fate and kinetics of tritium-labeled substrates were determined by HPLC-LSC analysis of products.

R-[6-^{3}H]-CH_2H_4folate. The *R*6 hydrogen of CH_2H_4folate is the source of the hydride that reduces the exocyclic methylene intermediate in classical TSs (*1*). Thus, its reaction with *R*-[6-^{3}H]-CH_2H_4folate leads exclusively to tritiated dTMP (*6, 11*). Here, we conducted the reaction with FDTS under strict anaerobic conditions, using 5 mM formaldehyde (to convert the unstable H_4folate product to CH_2H_4folate). The tritium remained on the *R*-[6-^{3}H]-CH_2H_4folate even when all dUMP was converted to dTMP (as followed by the conversion of the [2-^{14}C]-dUMP to [2-^{14}C]-dTMP). The anaerobic conditions were required because under aerobic conditions some H_2folate was formed (as detected by the UV chromatogram and tritium radiogram).

S-[4-^{3}H]-NADPH. Experiments with *S*-[4-^{3}H]-NADPH showed that the pro-*S* tritium remained exclusively on the $NADP^+$ product (*16*), which suggests that the FDTS is predominantly an *R*-specific protein.

R-[4-^{3}H]-NADPH. The experiments were repeated with *R*-[4-^{3}H]-NADPH, and the tritium from the 4*R* position of NADPH was transferred very slowly (relative to the conversion of the ^{14}C) to water and $NADP^+$ (*16*). This indicates that (i) the hydride is not transferred directly from NADPH to reduce the methylene since no tritium was detected in the dTMP product, (ii) the oxidation of NADPH is not strictly stereospecific although the *R* is clearly preferred. We suggest that due to the large kinetic isotope effect (KIE) on the tritium abstraction from the *R* position, some *S*-protium is also abstracted, which leads to tritium in the $NADP^+$ product.

A primary (1°) KIE can be estimated from $\ln(1 - f_{14})/\ln(1 - f_T)$ (*17*), where f_{14} is the fractional conversion for the ^{14}C (representing conversion of the protonated NADPH) and f_T is the fractional conversion for the tritiated NADPH to water. Calculation of f_{14} is straightforward:

$$f_{14} = \frac{dTMP_{14}}{dTMP_{14} + dUMP_{14}} \quad (1)$$

where $dUMP_{14}$ and $dTMP_{14}$ represent the integrated radioactivity (dpm) measured for the reactant and the product. Since the enzyme is not 100% stereospecific, calculation of the f_T requires estimation of the portion of *R*-[4-^{3}H]-NADPH that is bound to form tritiated water (1°). This is possible by using the reasonable assumption that the secondary (2°) KIE is close to unity, so the fractional conversion of [4-^{3}H]-$NADP^+$ from *R*-[4-^{3}H]-NADPH is close to f_{14}, and

$$f_T = \frac{H_2O_T}{H_2O_T + (NADPH_T - NADP^+_T(1 - f_{14}))} \quad (2)$$

where H_2O_T, $NADPH_T$, and $NADP_T^+$ represent the integrated radioactivity (dpm) measured for each material. The tritium in water is corrected for as described above for the *S*-[4-^{3}H]-NADPH. This calculation yields a 1° KIE between 19 and 31 (25 ± 6). This KIE was measured via competition between tritiated and protonated substrates and thus is the observed KIE on the second-order rate constant (*V/K*) of the enzyme (*18*, *19*). This is a very large observed KIE and indicates that hydride transfer is the rate-limiting step (see also the FAD reduction experiment below). Additionally, this KIE is much larger than that predicted by semiclassical calculations and is consistent with a possible contribution of quantum mechanical hydrogen tunneling to the C−H−N transfer from the pro-*R* C-4 of NADPH to the N-5 of the flavin (*17*, *18*, *20*, *21*).

D_2O Study. To identify the source of the hydride that reduces the methylene intermediate, a "cold" reaction mixture (no radioactive material was added to the reaction mixture, see Methods) containing about 50% D_2O was analyzed using electron spray mass spectrometry (ESMS). The mass spectrum (*16*) revealed the existence of a molecular ion peak of monodeuterated dTMP at $m/z = 322$. This peak serves as evidence of the incorporation of deuterium from the solvent into the methyl group of the dTMP. Protonic-exchange processes between reduced flavin (N-5 is a basic secondary amine in the $FADH_2$ state) and water protons are very fast (10^3−10^7 s^{-1} (*22*)). Such exchange is well established and, to the best of our knowledge, was first demonstrated by Delk et al. (*22*) for the folate-dependent ribothymidyl synthase. However, it is worth mentioning that the mechanistic features of ribothymidyl synthase are apparently different from FDTS. One important distinction between the two proteins is that in FDTS the flavin (FAD) is tightly bound to the enzyme and NADPH is the reducing agent, whereas in ribothymidyl synthase, the $FMNH_2$ is the reducing agent in a sequential mechanism.

Our above findings on FDTS, taken together with the fact that no tritium incorporation into the dTMP product was detected when using tritiated NADPH (*16*), indicate that following FAD reduction, the $FADH_2$ protium exchange with water must precede its oxidation by the methylene intermediate.

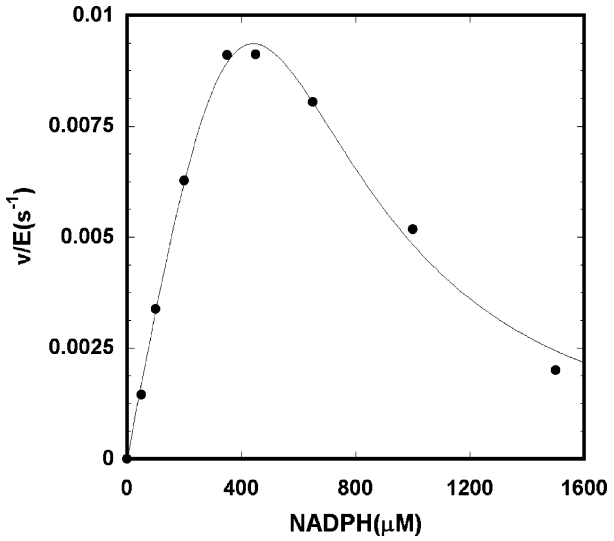

FIGURE 1: Steady-state initial velocity rates vs NADPH concentration at 100 μM dUMP and 500 μM CH_2H_4folate. The line is the nonlinear root-mean-square fit to eq 3.

Enzyme−FAD Reduction by NADPH. To test whether NADPH reduction precedes the binding of dUMP and CH_2H_4folate and thus the feasibility of a ping-pong mechanism, we incubated the enzyme-bound FAD (2.4 μM) with excess NADPH (1 mM) in 200 mM Tris buffer, pH = 8, under Ar. The UV spectrum of that mixture clearly indicated slow but complete reduction of the FAD to $FADH_2$ (*16*). On the other hand, the spectra of the reaction mixture showed decreasing 340 nm absorbance (due to oxidation of NADPH) but no change in the FAD 454 nm absorbance throughout the course of the reaction (consistent with the yellow color of the reaction mixture at all times). Taken together, this suggests that the NADPH binding precedes binding of the other reactants and that the FAD reduction step is rate-limiting for the overall catalytic cascade, leading to accumulation of the oxidized enzyme−FAD complex at a steady-state concentration close to the total enzyme concentration. This conclusion is also consistent with the large observed KIE on *V/K* under steady-state kinetics (see the *R*-[4-^{3}H]-NADPH experiment above).

NADPH Concentration Dependence of Initial Rates. The steady-state initial velocities were measured at 37 °C. NADPH concentrations were varied from 10 to 1500 μM with fixed dUMP concentration of 100 μM and 500 μM CH_2H_4folate. Variations in dUMP and CH_2H_4folate had no effect on the rates, suggesting that these substrate were saturating under these conditions. The initial velocities were divided by the enzyme concentration. The results are presented in Figure 1 and indicate that substrate inhibition decreased the rates at high NADPH concentrations. The data were best fitted to eq 3 (uncompetitive substrate inhibition) (*23*).

$$v = k_{cat}[S]/(K_M + [S](1 + [S]/K_S)) \quad (3)$$

where [S] is the NADPH concentration, k_{cat} is the first-order rate constant, K_M is the Michaelis constant, and K_S is the substrate inhibition constant. The lines represent the nonlinear fit of the data to eq 3. The fitting results in k_{cat} of 0.1 s^{-1}, $K_M = 4$ mM, and $K_S = 40$ mM. A quantitative assay for FDTS has been reported for the first time very recently (*5*).

Unfortunately, their assay followed the tritium release from [5-^{3}H]-dUMP under inhibitory concentration of NADPH as apparent from Figure 1. The new method presented here has an additional advantage because it uses DTT instead of β-mercaptoethanol, which is known to trap the putative methylene intermediate (*24*).

Docking and Modeling. Crystal structures of FDTS with NADPH or CH_2H_4folate are not yet available. To test the structural feasibility of various proposed complexes along the reaction path suggested below, these complexes were modeled into the structure of TM0449. Both models were based on the recently reported coordinates of the TM0449 complex with FAD and dUMP (PDB entry 1O26) (*3*).

(a) NADPH. Since our findings suggest that NADPH can bind the enzyme−FAD complex prior to dUMP binding, we replaced the dUMP coordinates with the nicotinamide ring of NADPH and minimized the new complex. After minimization, the nicotinamide fits into the dUMP binding site with its C-4 only 3.5 Å from the N-5 of the flavin. Another interesting feature of this docking model is that when the pro-*R*4 hydrogen of the nicotinamide is facing the flavin, its carbonyl and amide are in a cavity surrounded by Ser88, Arg147, and the backbone carbonyl of Leu87. All of these functional groups can form hydrogen bonds with the amide and stabilize that conformation. This could explain the preferred (though not absolute) stereospecificity of the enzyme toward the *re* face of the nicotinamide moiety.

(b) CH_2H_4folate. CH_2H_4folate is the only possible source of single carbon (methylene) in the FDTS reaction and has to be bound in close proximity to the C-5 of dUMP. As indicated before, CH_2H_4folate cannot fit into the FAD binding pocket (*3*), and the option of FAD replacement by means of CH_2H_4folate binding close to the dUMP is not realistic. The FAD is tightly bound to the enzyme throughout the catalytic cycle (through its adenine-pyrophosphate anchor), yet its flexible isoalloxazine ring can be distorted to accommodate the pterin moiety of CH_2H_4folate. The modeling of CH_2H_4folate in complex with a distorted FAD and dUMP is presented in Figure 2. The isoalloxazine ring is replaced by the pterin (also see Scheme 1) where the dUMP occupies the same conformation as in the original crystal structure, and the C-5 of dUMP is 3.7 Å from the diazoformylacetal moiety of the CH_2H_4folate. The proposed 2′−3′ rotation of the ribityl moiety of FAD that moved the isoalloxazine ring out of its binding site is similar to that found in other flavo-enzymes (*13*−*15*). Actually, even greater flexibility is anticipated in this surface-exposed active site, so Ser88 could nucleophilically attack C-6 of dUMP (*3*). The (*p*-aminobenzoyl)-glutamate moiety of the CH_2H_4folate does not interact with the interior of the enzyme (see Scheme 1 and Figure 2).

CONCLUSIONS

The reaction mechanism of a FDTS (TM0449 encoded by *Thy1* from *T. maritima*) was studied. The findings indicated that (i) the pro-*R* hydride of a nicotinamide (NADPH) and not the *R*6 hydride of the tetrahydropterin (CH_2H_4folate) is the reducing agent, (ii) the stereospecificity for the pro-*R* NADPH oxidation is not absolute, (iii) this hydride is transferred to FAD, which is the overall rate-limiting step of the catalytic cascade, (iv) this reduction precedes, and does not require, any other substrate binding, (v) large 1° KIE is in accordance with quantum mechanical hydrogen tunneling, (vi) the reduced $FADH_2$ exchanges its N-5 proton with the solvent prior to hydride transfer from that position to the methylene intermediate (which is formed by methylene transfer from CH_2H_4folate to dUMP), (vii) H_4-folate and not H_2folate is indeed the product of this reaction, and (viii) substrate inhibition, low k_{cat}, and large K_M may rationalize the slow activity previously reported (*3*−*5*).

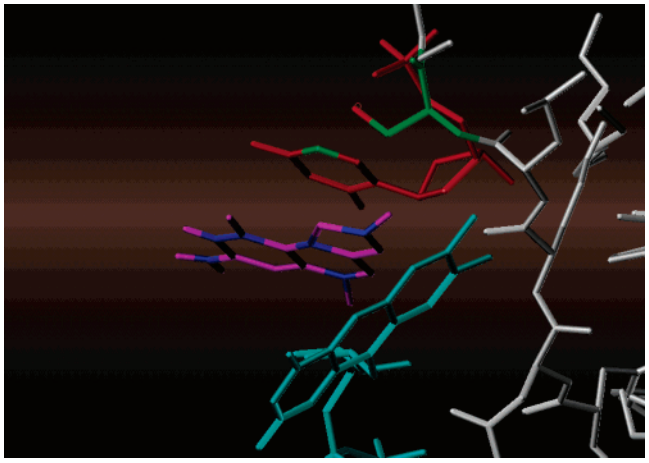

FIGURE 2: A possible TM0449−FAD−dUMP−CH_2H_4folate reactive complex. The methylated pterin (magenta) is in the original binding pocket of the flavin (PDB no. 1O26) as illustrated in Scheme 1. dUMP (red) and Ser88 (green) occupy their original coordinates. The flavin (cyan) is shifted by rotation of a single bond as described in the text. Highlighted atoms are the nitrogen atoms of the pterin ring (blue), the C-5 position of dUMP (green-blue), and the active oxygen of Ser88 (red), which is the presumed enzymatic nucleophile.

Scheme 2: The Proposed Order of Substrate Binding and Product Release during the Catalytic Cycle of FDTS (Uni Uni Bi Bi Ping-Pong, see text)[a]

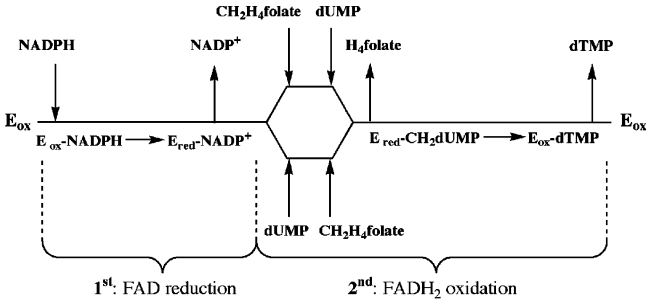

[a] The reaction can by divided into two half-reactions: 1st, a slow reduction of FAD and 2nd, a fast methylene transfer and reduction to yield products and oxidized FAD.

In accordance with all of these experimental observations, Scheme 2 suggests a sequential Uni Uni Bi Bi Ping-Pong mechanism (*25*) for the binding of substrates and the release of products. The first half-reaction includes the binding of NADPH and the release of the $NADP^+$. The second half-reaction includes random or ordered binding of dUMP and CH_2H_4folate and ordered release of H_4folate followed by dTMP. This mechanism contrasts with the Bi Bi ordered mechanism of the classical TS, where ordered binding of dUMP and CH_2H_4folate is followed by ordered release of H_2folate and dTMP (*1*, *6*).

Scheme 3: The Proposed Chemical Mechanism for the FDTS Catalyzed Reaction[a]

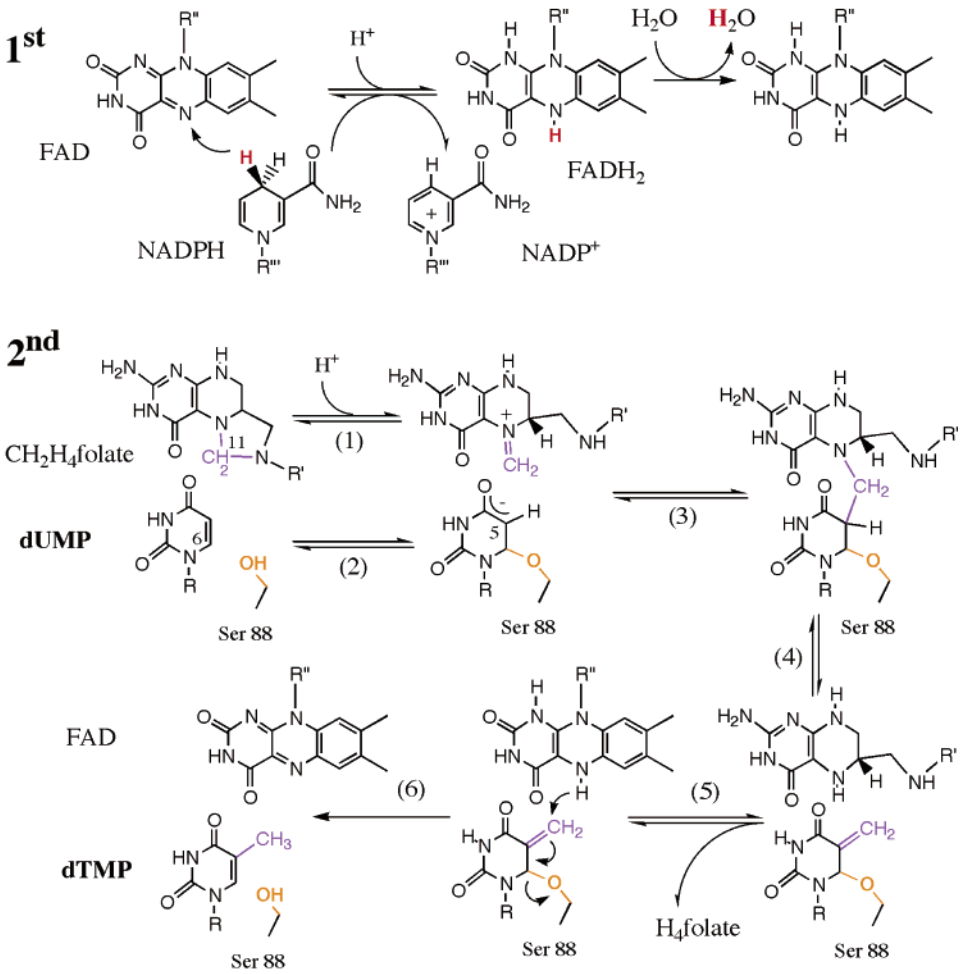

[a] The hydride is in red, the enzymatic nucleophile in yellow, and the methylene in purple. R = 2′-deoxyribose-5′-phosphate, R′ = (*p*-aminobenzoyl)-glutamate, R″ = adenosine-5′-pyroposphate-ribityl, R‴ = 2′-phospho-adenosine-5′-pyrophosphate-ribose.

Consistent with this binding mechanism, molecular details of the proposed mechanism are illustrated in Scheme 3. Initially NADPH binds, reduces the yellow FAD to a colorless $FADH_2$, and releases $NADP^+$ (Scheme 3, 1st). The reduced and solvent-exposed enzyme−$FADH_2$ exchanges protium with the solvent before (or while) binding dUMP and CH_2H_4folate in a sequential fashion (random or ordered). The CH_2H_4folate binding requires a conformational change of the isoalloxazine ring but not the release of the entire FAD. The dUMP is activated by nucleophilic attack at its C-6 position (probably by Ser88 (*3*−*5*)) and CH_2H_4folate transfers its methylene group to the C-5 dUMP (Scheme 3, 2nd, step 3). Then, elimination of H_4folate forms the exocyclic methylene intermediate (step 4). The H_4folate is then released and the isoalloxazine ring of the flavin flips-in (step 5) and reduces the exocyclic methylene−dUMP intermediate, leading to release of the final product (dTMP) and an enzyme−FAD complex that is ready for another turnover (step 6). The first half-reaction and steps 5 and 6 of the second half-reaction are well supported by the experimental findings. Steps 1−4 of the second half-reaction are suggested by analogy to the TS reaction (*1*) and are supported by structural and mutational findings (*3*−*5*). It is not clear from the modeling why the unstable H_4folate does not transfer its C-6 hydride to the exocyclic methylene intermediate (which would be thermodynamically favored and is mandatory in the classical TS reaction). In contrast to a thiol in the classical TS reaction (e.g., Cys146 in *Escherichia coli*), a hydroxyl (e.g., Ser88 or Ser84 in *H. pylori*) is the most likely activator of the C-6 position of dUMP. The methylene reduction may be concerted with the leaving of the nucleophile (hydroxylate or thiolate) of the enzyme and proceed via a 1,3-S_N2-like substitution (Scheme 3, step 6, see arrows for relevant electron flow). In such a case, the energetic difference between the more stable ether bond and the less stable classic thioether bond may explain why the hydride from the H_4-folate (tetrahydropterin) cannot be transferred and a more nucleophilic hydride (such as that of N-5 of $FADH_2$) is needed.

Uncompetitive substrate inhibition of NADPH was observed while measuring the steady-state rate constants and may explain the low activity of the enzyme at high nicotinamide concentration in the past (*3*−*5*). In fact, ref *5* conducted all assays in 2 mM NADPH at which the observed rate is much lower than at 0.5 mM (see Figure 1) and is by an order of magnitude lower than k_{cat}, which takes into consideration the NADPH inhibition (0.007 vs 0.1 s^{-1} for their observed rate vs our fitted k_{cat}, respectively). The low k_{cat} and the large K_M (0.1 s^{-1} and 4 mM, respectively) may suggest that NADPH is not the natural reductant. Experiments that attempt to identify an alternative natural reductant are underway.

FDTSs are critical to the survival of several pathogenic bacteria that lack *ThyA*, DHFR, and thymidine kinase (*3*, *4*). The findings presented here indicate a substantially different kinetic and chemical mechanism for FDTS than that for human and other classical TSs. These findings further invoke the notion that FDTS is a most attractive target for designing specific antibiotic drugs against many diseases such as syphilis, ulcers, periodontal disease, Lyme's disease, and more (*3*) and biological warfare agents such as anthrax, botulism, and typhus. We hope that the results reported here may provide the impetus for further structural and mechanistic studies that, when combined with kinetic data, should provide detailed insight into this intriguing class of enzymes.

ACKNOWLEDGMENT

We thank Dr. Rudolf Moser, Eprova, Switzerland, for the generous gift of nonradioactive CH_2H_4folate, and Dr. Lynn Teesch and the Center for Mass Spectrometry at the University of Iowa for the ESMS analysis. We also thank Drs. Paul Fitzpatrick, John Blanchard, Judith Klinman, and Richard Schowen for useful discussions.

SUPPORTING INFORMATION AVAILABLE

Experimental details, raw data, radiograms, and MS and UV/vis spectra. This material is available free of charge via the Internet at http://pubs.acs.org.

REFERENCES

1. Carreras, C. W., and Santi, D. V. (1995) The catalytic mechanism and structure of thymidylate synthase, *Annu. Rev. Biochem. 64*, 721−762.
2. Finer-Moore, J. S., Santi, D. V., and Stroud, R. M. (2003) Lessons and conclusions from dissecting the mechanism of a bisubstrate enzyme: thymidylate synthase mutagenesis, function and structure, *Biochemistry 42*, 248−256.
3. Mathews, I. I., Deacon, A. M., Canaves, J. M., McMullan, D., Lesley, S. A., Agarwalla, S., and Kuhn, P. (2003) Functional analysis of substrate and cofactor complex structures of the thymidylate synthase-complementing protein, *Structure 11*, 677−690.
4. Myllykallio, H., Lipowski, G., Leduc, D., Filee, J., Forterre, P., and Liebl, U. (2002) An alternative flavin-dependent mechanism of thymidylate synthesis, *Science 297*, 105−107.
5. Leduc, D., Graziani, S., Lipowski, G., Marchand, C., Le Maréchal, P., Liebl, U., and Myllykallio, H. (2004) Functional evidence for active site location of tetrameric thymidylate synthase X at the interphase of three monomers, *Proc. Natl. Acad. Sci. U.S.A. 101*, 7252−7257.
6. Agrawal, N., Hong, B., Mihai, C., and Kohen, A. (2004) Vibrationally enhanced hydrogen tunneling in the *E. coli* thymidylate synthase catalyzed reaction, *Biochemistry 43*, 1998−2006.
7. Stroud, R. M., and Finer-Moore, J. S. (2003) Conformational dynamics along an enzymatic reaction pathway: Thymidylate Synthase, "the Movie", *Biochemistry 42*, 239−247.
8. Kuhn, P., Lesley, S. A., Mathews, I. I., Canaves, J. M., Brinen, L. S., Dai, X., Deacon, A. M., Elsliger, M. A., Eshaghi, S., Floyd, R., Godzik, A., Grittini, C., Grzechnik, S. K., Guda, C., Hodgson, K. O., Jaroszewski, L., Karlak, C., Klock, H. E., Koesema, E., Kovarik, J. M., Kreusch, A. T., McMullan, D., McPhillips, T. M., Miller, M. A., Miller, M., Morse, A., Mon., K., Ouyang, J., Robb, A., Rodrigues, K., Selby, T. L., Spraggon, G., Stevens, R. C., Taylor, S. S., Van den Bedem, H., Velasquez, J., Vincent, J., Wang, X., West, B., Wolf, G., Wooley, J., and Wilson, I. A. (2002) Crystal structure of thy1, a thymidylate synthase complementing protein from thermotoga maritima at 2.25 Å resolution, *Proteins: Struct., Funct., Genet. 49*, 142−145.
9. McCracken, J. A., Wang, L., and Kohen, A. (2003) Synthesis of R and S tritiated reduced b-nicotinamide adenine dinucleotide 2′ phosphate, *Anal. Biochem. 324*, 131−136.
10. Markham, K. A., Sikorski, R. S., and Kohen, A. (2003) Purification, analysis and preservation of reduced nicotinamide adenine dinucleotide 2′-phosphate, *Anal. Biochem. 322*, 26−32.
11. Agrawal, N., Mihai, C., and Kohen, A. (2004) Microscale Synthesis of isotopically labeled R-[6-^{x}H]-N5, N10-methylene 5,6,7,8-tetrahydrofolate as a substrate for thymidylate synthase, *Anal. Biochem. 328*, 44−50.
12. Agrawal, N., and Kohen, A. (2003) Microscale synthesis of 2-tritiated isopropanol and 4-R tritiated reduced nicotinamide adenine dinucleotide phosphate, *Anal. Biochem. 322*, 179−184.
13. Gatti, D. L., Palfey, B. A., Soo Lah, M., Entsch, B., Massey, V., Ballou, D. P., and Ludwig, M. L. (1994) The mobile flavin of 4-OH benzoate hydorxylase, *Science 266*, 110−114.
14. Fitzpatrick, P. (2001) Substrate dehydrogenation by flavoproteins, *Acc. Chem. Res. 34*, 299−307.
15. Bruice, T. C. (1980) Mechanisms of Flavin Catalysis, *Acc. Chem. Res. 13*, 256−162.
16. See Supporting Information.
17. Melander, L., and Saunders, W. H. (1987) *Reaction rates of isotopic molecules*, R. E. Krieger, Malabar, FL.
18. Kohen, A. (2003) Kinetic isotope effects as probes for hydrogen tunneling, coupled motion and dynamics contributions to enzyme catalysis, *Prog. React. Kinet. Mech. 28*, 119−156.
19. Cleland, W. W. (1991) Multiple isotope effects in enzyme-catalyzed reactions, in *Enzyme Mechanism from Isotope Effects* (Cook, P. F., Ed.) pp 247−268, CRC Press, Boca Raton, FL.
20. Bell, R. P. (1980) *The tunnel effect in chemistry*, Chapman & Hall, London and New York.
21. Kohen, A., and Klinman, J. P. (1998) Enzyme catalysis: beyond classical paradigms, *Acc. Chem. Res. 31*, 397−404.
22. Delk, A. S., Nagle, D. P., Jr., and Rabinowitz, J. C. (1980) Methylenetetrahydrofolate-dependent biosynthesis of ribothymidine in transfer RNA of *Streptococcus faecalis*, *J. Biol. Chem. 255*, 4387−4390.
23. Charlier, H. A., Jr., and Plapp, B. V. (2000) Kinetic cooperativity of human liver alcohol dehydrogenase, *J. Biol. Chem. 275*, 11569−11575.
24. Barrett, J. E., Maltby, D. A., Santi, D. V., and Schultz, P. G. (1998) Trapping of the C5 methylene intermediate in thymidylate synthase, *J. Am. Chem. Soc. 120*, 449−450.
25. Cleland, W. W. (1979) Statistical analysis of enzyme kinetic data, *Methods Enzymol. 63*, 103−138.

BI0490439